A Novel Method for Vibrotactile Proprioceptive Feedback Using Spatial Encoding and Gaussian Interpolation

A Novel Method for Vibrotactile Proprioceptive Feedback Using Spatial Encoding and Gaussian Interpolation

Marinelli, A; Boccardo, N; Canepa, M; Domenico, D Di; Semprini, M; Chiappalone, M; Laffranchi, M; De Michieli, L; Dosen, S

Published in:
I E E E Transactions on Biomedical Engineering

DOI (link to publication from Publisher):
10.1109/TBME.2023.3285850

Publication date:
2023

Document Version
Accepted author manuscript, peer reviewed version

A Novel Method for Vibrotactile Proprioceptive Feedback Using Spatial Encoding and Gaussian Interpolation

A. Marinelli, *Student Member*, *IEEE*, N. Boccardo, M. Canepa, D. Di Domenico, *Student Member*, *IEEE*, M. Semprini, *Member*, *IEEE*, M. Chiappalone, *Member*, *IEEE*, M. Laffranchi, *Member*, *IEEE*, L. De Michieli, *Member*, *IEEE*, S. Dosen, *Member*, *IEEE*

***Abstract*— *Objective:* The bidirectional communication between the user and the prosthesis is an important requirement when developing prosthetic hands. Proprioceptive feedback is fundamental to perceiving prosthesis movement without the need for constant visual attention. We propose a novel solution to encode wrist rotation using a vibromotor array and Gaussian interpolation of vibration intensity. The approach generates tactile sensation that smoothly rotates around the forearm congruently with prosthetic wrist rotation. The performance of this scheme was systematically assessed for a range of parameter values (number of motors and Gaussian standard deviation). *Methods*: Fifteen able-bodied subjects and one individual with congenital limb deficiency used vibrational feedback to control the virtual hand in the target-achievement test. Performance was assessed by end-point error and efficiency as well as subjective impressions. *Results*: The results showed a preference for smooth feedback and a higher number of motors (8 and 6 versus 4). With 8 and 6 motors, the standard deviation, determining the sensation spread and continuity, could be modulated through a broad range of values (0.1 - 2) without a significant performance loss (error: ~ 10%; efficiency: ~ 30%). For low values of standard deviation (0.1-0.5), the number of motors could be reduced to 4 without a significant performance decrease. *Conclusion:* The study demonstrated that the developed strategy provided meaningful rotation feedback. Moreover, the Gaussian standard deviation can be used as an independent parameter to encode an additional feedback variable. *Significance:* The proposed method is a flexible and effective approach to providing proprioceptive feedback while adjusting the trade-off between sensation quality and the number of vibromotors.**

***Index Terms*—Gaussian interpolation, Haptics, Multichannel stimulation, Proprioception, Prosthesis, Spatial encoding, Vibrotactile stimulation.**

I. Introduction

OVER the past twenty years, the field of multi-functional upper limb prostheses was marked with important technological and scientific developments aiming to better satisfy the needs of prosthesis users. The loss of an upper limb is a traumatic event with a strong impact on the ability to participate in the activities of daily living [1, 2], thereby leading to a substantial decrease in the quality of life [3]. Despite the aforementioned developments, in a recent study, Salminger, et al. [4] reported overall abandonment rates of about 44% for the users of upper limb myoelectric prostheses. An important drawback of modern prostheses is that they lack explicit somatosensory feedback. Without the feedback, the user can still estimate the state of the device using incidental cues, such as visual observation and motor sound [5, 6], but this requires constant attention to the prosthesis. Providing explicit feedback can reduce cognitive load and fatigue when using prostheses [2, 7].

To mitigate this drawback, methods to restore the missing sensory information were proposed in the literature, and the results demonstrated that the artificial sensory feedback can enrich the prosthesis-user interaction by improving performance [8-10] and subjective experience [11, 12] as well as by facilitating the feeling of embodiment [13-15]. Reestablishing the closed-loop control, characteristic of sound limbs, can trigger somatosensory plasticity and promote long-term learning and adaptation processes for artificial sensations [16].

To provide sensory feedback, the information about the prosthesis state can be conveyed to the subject invasively [17-21], by electrically stimulating peripheral nerves that innervated the lost hand, or non-invasively [7, 22-25], by delivering mechanical or electrical stimulation to the skin of the residual limb. Despite the invasive methods needing a surgical procedure to implant the electrodes, they allow providing somatotopic feedback, where the tactile sensation is experienced as coming from the missing limb (phantom

This work was supported in part by the Istituto Nazionale Assicurazione Infortuni sul Lavoro, under the project iHannes (PR19-PAS-P1) and in part by the Danish Independent Research Foundation, under the project ROBIN (8022-00243A). *Corresponding authors: A. Marinelli and S. Dosen.*

A. Marinelli is with the Istituto Italiano di Tecnologia and with the University of Genova, Genova, Italy (e-mail: andrea.marinelli@iit.it)

N. Boccardo is with the Istituto Italiano di Tecnologia, Genova, Italy (e-mail: nicolo.boccardo@iit.it)

M. Canepa is with the Istituto Italiano di Tecnologia, Genova, Italy (e-mail: michele.canepa@iit.it)

D. Di Domenico is with the Istituto Italiano di Tecnologia, Genova, Italy and with the Politecnico di Torino, Torino, Italy (e-mail: dario.didomenico@iit.it)

M. Semprini is with the Istituto Italiano di Tecnologia, Genova, Italy (e-mail: marianna.semprini@iit.it)

M. Chiappalone is with the University of Genova and with the Istituto Italiano di Tecnologia, Genova, Italy (e-mail: michela.chiappalone@iit.it)

M. Laffranchi is with the Istituto Italiano di Tecnologia, Genova, Italy (e-mail: matteo.laffranchi@iit.it)

L. De Michieli is with the Istituto Italiano di Tecnologia, Genova, Italy (e-mail: lorenzo.demichieli@iit.it)

S. Dosen is with the Aalborg University, Aalborg, Denmark (e-mail: sdosen@hst.aau.dk).

This article has been accepted for publication in IEEE Transactions on Biomedical Engineering. This is the author's version which has not been fully edited and content may change prior to final publication. Citation information: DOI 10.1109/TBME.2023.3285850

sensation) [26]. Such invasive feedback was used to convey pressure [27], textures [21], slippage [28], pain [17], and proprioception [7, 18]. However, this approach has several drawbacks including the risks of surgery, subject reluctance to undergo additional surgical operations, high cost, lack of access, and limitations in perceptual performance due to the difficulty in selective activation of target nerves. Non-invasive methods are simpler to implement and can be particularly relevant in those subjects that are reluctant to undergo further surgical procedures [29]. Although the non-invasive stimulation results in a less natural sensation (e.g., non-somatotopic), the subjects can quickly learn to interpret the feedback and integrate it into the body scheme [30]. In most studies, prosthesis grasping force was selected as the variable to be transmitted to the user [7, 8, 23-25, 31-35], while the artificial proprioceptive feedback, conveying the position of the prosthesis joints (e.g., wrist rotation and hand aperture), was seldom considered [22, 36-41].

Different methods have been presented in the literature to provide artificial proprioceptive feedback. The most natural approach is to induce a realistic kinesthetic illusion [38, 40, 42, 43], where a phantom sensation of the movement of the missing limb is created, for instance, by vibrating muscles to activate muscle afferents [44-46]. This is modality-matched feedback and hence likely most intuitive for the subject, but the setup can be cumbersome. Another approach that can be implemented using a more compact setup is the sensory substitution feedback, where proprioceptive information (e.g., wrist angle) is provided indirectly, using tactile stimulation [7]. In this approach, at least a brief training is required to teach the subject to associate the tactile sensation with the provided information. Tactile stimulation can be delivered mechanically (e.g., using vibration motors) or electrically, but regardless of the stimulation interface one of the critical questions when designing such feedback is the choice of the encoding scheme, which defines the mapping between the feedback variable and stimulation profile [7].

When a single-channel stimulation is used, the feedback information can be encoded by modulating stimulation parameters, such as intensity. A conventional approach would be to modulate the intensity or frequency of electro or mechanotactile stimulation [31, 47, 48]. Recently, Battaglia, et al. [38] and Kayhan, et al. [37] presented a novel solution to convey wrist rotation and/or hand aperture by stretching the skin. When multiple stimulation channels are available, feedback information can be conveyed also by changing the location of stimulation (active channel), the approach known as spatial encoding. Witteveen, et al. [49] used arrays of vibromotors or electrotactile stimulators to convey hand aperture feedback. In Garenfeld, et al. [50] wrist orientation and hand aperture information were provided using electrotactile stimulation delivered through a 16-pad electrode array. Finally, the most flexible scheme is to combine spatial encoding and parameter modulation, which is a so-called mixed encoding approach. For instance, Erwin and Sup IV [51] combined the spatial activation of three vibration motors with the modulation of vibration frequency to convey the position of a virtual wrist. Despite different methods have been used to encode the proprioceptive information, they are rarely compared against each other (see [36] for the comparison between spatial and amplitude schemes). In addition, the methods are usually implemented by heuristically predefining the configuration parameters (e.g., number of motors, intensity) instead of systematically investigating the performance across the parameter space. However, such comparisons are important as they can help to make informed choices when designing feedback interfaces.

The present study describes a novel approach to providing wrist rotation feedback using an array of vibromotors and a mixed encoding paradigm. Multiple vibrators were activated simultaneously to produce the moving phantom sensation, while the vibration intensity was interpolated across the array following the Gaussian profile. This approach provided a continuous sensation of motion around the forearm that was congruent with the motion of the prosthesis. In this scheme, the quality of the elicited sensations critically depends on the number of motors in the array as well as the “width” of the Gaussian. For instance, increasing the width makes the change in sensation around the forearm more smooth and hence continuous. In addition, decreasing the number of motors can simplify the integration of the feedback interface into the prosthetic socket. Such continuous feedback that directly follows the motion of a prosthesis would be intuitive and thereby easy to interpret (direct relation between sensation and feedback variable), could enable higher spatial resolution, and improve user experience by generating smooth and pleasant sensations [52]. These factors could in turn lead to more effective control and a decrease in the cognitive load and fatigue required to use a prosthesis. However, a “wider” Gaussian could also jeopardize the identification of the current wrist orientation conveyed by the momentary location of the peak of the Gaussian profile. In the present study, we have therefore investigated the impact of both of these factors on the effectiveness of vibrotactile feedback during the closed-loop control of a hand prosthesis. To this aim, the subjects performed a virtual target achievement test (TAC) [53], using a novel framework that simulates the behaviour of the Hannes prosthesis [54] while providing vibrotactile feedback to control the rotation of the virtual hand. The subjects performed the task with different combinations of the number of motors and Gaussian width, thereby systematically exploring the parameter space of the novel feedback approach. With the small width of the Gaussian, our method “reduces” to discrete spatial feedback used previously in the literature [46], where a single vibromotor is activated at a time (hence, localized stimulation which "jumps" around the forearm). Therefore, in addition to exploring the parameters, the present study also compares the conventional approach (discrete feedback) to the novel method that produces smooth sensations congruent to the orientation of the prosthesis.

II. Materials and Methods

A. Subjects

Fifteen healthy able-bodied subjects (aged 26.7 ± 3.2, 8 males), and an individual with congenital limb deficiency subject (aged 25, female) with no prior experience with proprioceptive tactile feedback, participated in this study.

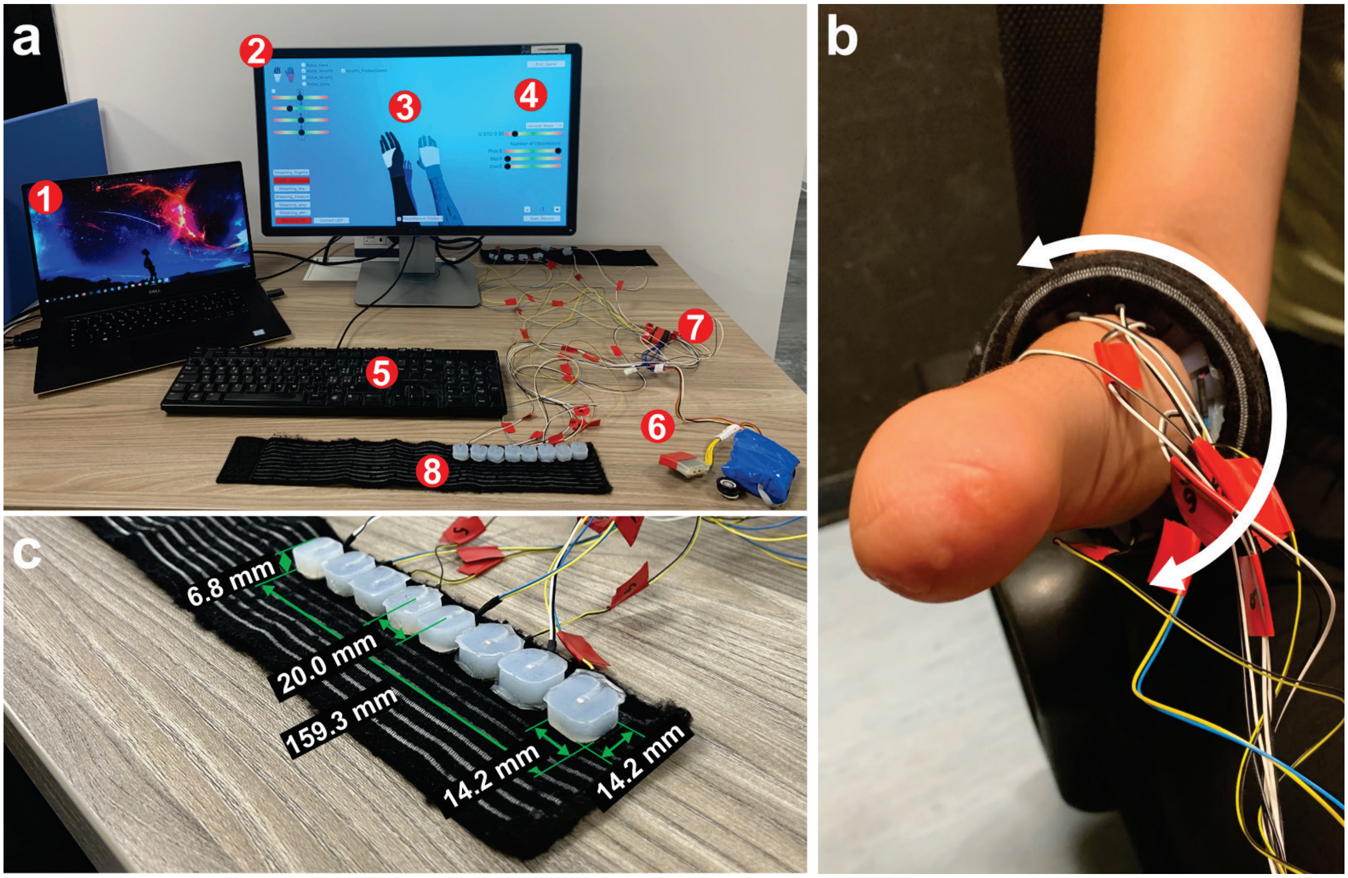

Figure 1 Experimental Setup. **a**: The subjects were seated in front of the monitor (2) wearing the armband with the vibromotors (8) placed equidistantly around the interior aspect of the right forearm. The virtual reality scenario showed the orientation of the target and the controlled hand (3). The graphical controls (4) allow for setting the parameters of the feedback scheme. The keyboard (5) was used to move the controlled prosthesis while its state (wrist angle) was conveyed through vibrotactile feedback. The setup also included a laptop (1), a master board with a battery pack (6), and a feedback control board (7). **b**: The elastic band with vibromotors placed around the medial part of the right forearm of an amputee participant. **c**: a detailed photo of the wristband with vibromotors with indicated dimensions.

Before starting the experiment, the subjects were informed about the protocol, and they signed the informed consent form. The experimental protocol was approved by the Research Ethics Committee of the Nordjylland Region (approval number N-20 190 036).

B. Experimental Setup

The experimental setup (Figure 1) comprised the following components: (i) a virtual reality (VR) environment simulating the Hannes prosthetic hand [54-57] with 3 active DoFs (hand open/close, wrist pronation/supination, and wrist flexion/extension), (ii) fourteen eccentric rotating mass vibromotors (Vybronics, VC0625B001L) with a custom-made control unit to provide tactile feedback, (iii) a custom-made master board to establish the communication between a host PC and feedback control unit, (iv) a battery pack, and (v) a standard laptop (DELL XPS 15, Intel Core i9 @2.60GHz, 32GB RAM) running Windows 10, an 18'' computer monitor and a keyboard. The master board communicated with the feedback controller using CAN Bus protocol, while it was connected to the laptop via Bluetooth. The VR framework was developed using the Unity development suite and C# language. The framework acquired the data from the master board and sent control commands to the feedback controller to generate desired vibrotactile stimulation.

As explained later (see section II.D), up to eight vibromotors were placed circumferentially and equidistantly around the subject's right forearm (see Figure 1.a and c), approximately 15 cm distal to the elbow, and strapped using an elastic band (Figure 1.c). Regardless of the number of motors used (i.e., 8, 6, 4), the first vibromotor was always placed in the middle at the volar side while the last was positioned in the middle of the dorsal side, covering thereby the half of the forearm (its internal portion). The rest of the motors were then placed equidistantly between the first and the last motor. This placement was selected because the spatial extent of the vibrotactile interface matched the range of motion of the virtual prosthesis and the elicited sensations were thereby congruent to the prosthesis motion. More specifically, the generated sensation indicated the position of the dorsal side of the prosthetic hand, as shown in Figure 3. Alternatively, the vibromotors could have been placed to cover the full circumference of the forearm. This would increase the spatial separation between the neighboring motors, potentially facilitating their discrimination, but the exact correspondence between the spatial configuration of the prosthesis and the forearm sensation would have been lost.

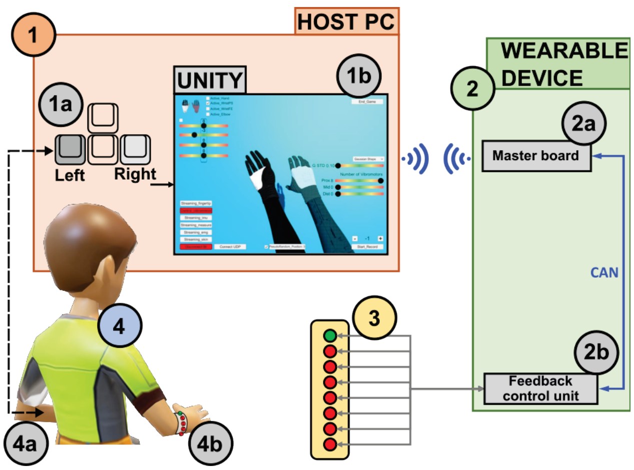

Figure 2 Closed-loop control of a virtual prosthesis. The subject controlled the rotation of the virtual hand by pressing on the keyboard (1a) with the left hand (4a). The Unity virtual environment (1b) visualized the target hand and recorded the trajectory performed by the controlled hand. The laptop (1) communicated via Bluetooth with the master board (2a) sending the feedback shape, while the master board, in turn, sent the commands to the feedback control unit (2b), which activated the vibromotors (3) to provide the feedback to the subject's right forearm (4b).

Only up to eight vibromotors, out of fourteen available, were used in the present study.

As noted in the introduction, the proposed approach provides feedback to the user by generating a specific intensity profile (Gaussian interpolation) that moves across multiple vibromotors. To be able to generate a well-controlled complex sensation, the elementary sensations elicited by a single motor need to be localized below the motor. Therefore, the vibromotors were covered with a soft silicone case to absorb the stimulation radiating from each motor. The case was thicker laterally (10mm) to separate two consecutive vibromotors while the side in contact with the skin was thin (1mm) to enable vibrations to be delivered effectively while avoiding the heating of the skin during prolonged motor activity. Finally, the silicon case allowed placing the vibromotors vertically to further spatially separate the consecutive motors and thereby allow the subjects to better detect the transitions between active motors. Vertical placement also provides a stronger sensation as shown in the pilot test that we conducted. The center-to-center distance between the consecutive motors is 20 mm, which is within the ranges of the two-point discrimination (2PD) thresholds reported in the literature [58]. However, for our encoding approach, it is not critical that the motors are separated by the 2PD. This is because the subjects do not need to recognize the activation of a random motor (absolute recognition); instead, they can rely on detecting the smooth transitions between active motors (relative recognition), as explained in section II.C.

The silicone case had a Velcro on top to be fixed to the elastic band, to prevent slips. The elastic band was strapped to the subject forearm with Velcro by applying the level of pressure which was enough to hold the motors securely in place, without masking the vibration sensation and/or constricting blood flow. To check the tightness, the subject was asked to rotate the

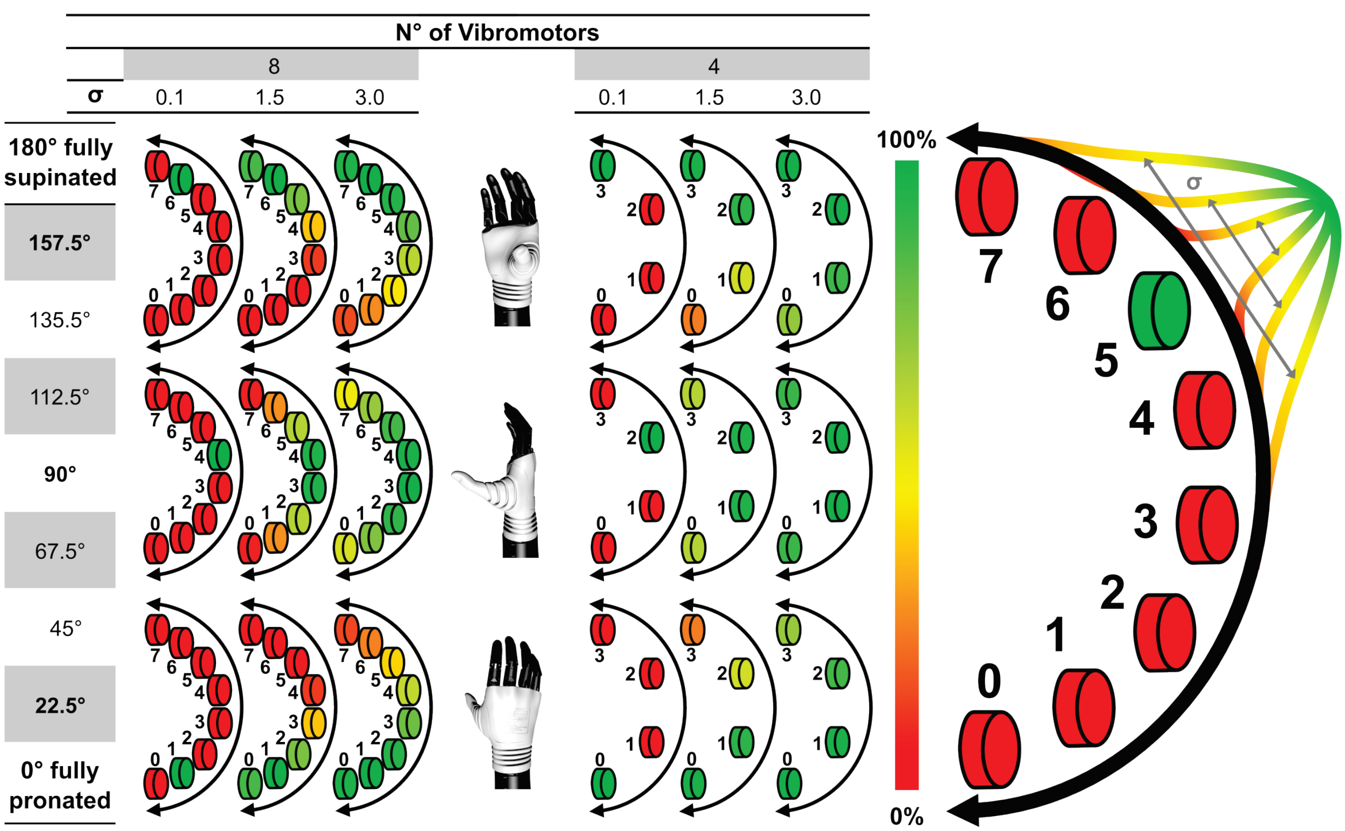

Figure 3 Illustration of the novel feedback encoding approach. The left panel displays three wrist positions and the corresponding stimulation profiles (vibration intensity across motors) generated for the different numbers of motors (8 or 4) and values of standard deviation (σ) of the Gaussian profile. The representation on the right shows the concept: a Gaussian profile with variable width (standard deviation parameter) that "rotates" around the forearm.

forearm, and if the elastic band moved accordingly without slipping, the band was deemed tight enough. The appropriate level of tightness was additionally confirmed during the calibration phase by checking that the sensation thresholds were not excessively high (compared to those obtained during pilot tests).

For each vibromotor, the vibration frequency was set to 200Hz using a supply voltage of 2.5V [59], which lay within the range of maximum sensitivity of the Pacinian corpuscles [60]. The gain of each vibromotor was individually adjusted for every subject (see section II.D).

Despite the virtual hand implementing 3 DoFs, only wrist rotation was controlled in the present study. The subject controlled the prosthesis movements using the keyboard and contralateral hand ("3" key for pronation, "4" key for supination). Such a setup provided reliable control and focused the subjects' attention on the feedback, ensuring thereby that the results reflected the changes in the feedback parameters (σ and the number of motors) rather than the influence of control strategy (e.g., changes in sensation due to movement of the forearm). The subjects sat comfortably in front of the monitor, with their right arm relaxed over the desk, taking care to avoid contact between the vibromotors and the table. The computer monitor was placed approximately 50 cm from the subject. The VR environment displayed two prosthetic hands, where one showed the target position (Figure 2.1b, transparent) while the other was controlled by the subject (Figure 2.1b, solid).

C. Vibrotactile feedback encoding

A novel encoding scheme was implemented to provide proprioceptive feedback (Figure 3). The rotation angle of the prosthesis wrist was conveyed to the subject by modulating both vibration intensity and location. To convey feedback that is spatially congruent to the prosthesis movement, a Gaussian profile of vibration intensity was "rotated" around the forearm in synchrony with the rotation of the hand (Figure 3, right). More specifically, the location of the profile peak always matched the orientation of the wrist, i.e., the Gaussian was centered at the first vibromotor (volar side) when the wrist angle was 0° (wrist starting orientation, completely pronated), then gradually moved across the vibromotors, to reach the last vibromotor (dorsal side) for the wrist angle of 180° (wrist end orientation, completely supinated). Interpolating the intensity using a "rotating" Gaussian function elicited a smooth sensation that was gradually moving around the forearm, thereby replicating a smooth movement of the prosthetic hand.

The following equation was used to define the Gaussian mapping between wrist orientation and vibration intensity:

$$\begin{cases} y = e^{-\frac{(k-m)^2}{g*\sigma^2}} \\ m = p*N \end{cases} \quad (1)$$

where y is the normalized vibration amplitude of the motor k, m is the mean of the Gaussian computed as the normalized position (p) of the virtual hand multiplied by the number of motors (N) in the array, g is a parameter set to 2.25, and σ is the standard deviation of the Gaussian. Effectively, m determines the location of the peak of intensity within the array of vibration motors while σ adjusts the spread of intensity across the motors. The interpolation function (1) can be used to define the mapping for different numbers of motors in the array, as determined by the parameter (N). The effect of the different number of vibromotors and the values of σ is visualized in Figure 3. In general, the σ adjusts the level of interpolation across the given number of motors thereby generating a more discrete or continuous sensation of movement around the forearm.

D. Experimental protocol

First, the minimum and maximum amplitude for each vibromotor were determined using the method of limits [61]. To this aim, the vibration intensity was increased in small steps (i.e., 4-5% in the normalized scale of pulse width modulation (PWM)). When the subject reported a sensation or discomfort felt for the first time, the momentary PWM was adopted as the sensation and discomfort threshold, respectively. This procedure is standardly performed to compensate for the individual perceptual abilities, and in this case, the possible differences in the tightness of the band holding the motors against the forearm. During the rest of the experiment, the vibration intensity was then modulated between these two thresholds, to generate clearly perceivable and localized vibrations that were not intrusive to the subject.

The subjects then performed the main experimental task, namely the target achievement test (TAC) [53]. They used the keyboard to rotate the virtual prosthesis to bring it into the target orientation (desired rotation angle). Importantly, the hand indicating the target position was always shown on the screen, whereas the hand controlled by the subject was not visible while the subject performed the task. At the beginning of each trial, both hands were visible thereby showing the target orientation and the starting position of the controlled hand. When the trial started, the controlled hand disappeared, and its momentary wrist angle was then conveyed to the subject through vibrotactile feedback. To ensure minimally intrusive feedback and avoid adaptation to stimulation, the vibration was provided only while subjects pressed the control keys, otherwise, the vibration was deactivated. The subjects were asked to press the space bar key when they thought to have reached the correct position. At that moment, the controlled hand was revealed to the subjects (however, the vibration was deactivated) so that they could see the deviation from the target rotation angle. This was done to increase the subjects' motivation during the experiment.

Each subject performed the task in 21 conditions, i.e., using 8, 6, and 4 vibromotors × 7 values of σ (0.1 – 3, in steps of 0.5). These values were determined heuristically and via pilot tests. For instance, the maximum number of vibromotors was set to 8 as this was the highest number that could be reasonably fitted around half of the forearm in most people. The minimum standard deviation was set to the value (0.1) that elicited discrete motor activation (hence discrete feedback). The other values were selected so that the parameter space was well explored while still maintaining a reasonable overall duration of the experimental session. In each condition, the subjects first received a short training to associate the new sensation scheme to the hand orientation. We also asked the subjects if the sensations were clear, to further check that they received the correct feedback, and that the sensation was not affected by adaptation during the experiment. Although the adaption was not explicitly measured, it is highly unlikely that it had an impact on the results of the present study, as the stimulation profiles were dynamic (varying in both intensity and position) and they were delivered intermittently [62]. Indeed, none of the subjects complained about the loss of sensations during the experiment. The virtual prosthesis was programmed to rotate back and forth, 5 times through the full range of motion. On this occasion, the controlled hand was visible to allow the subjects to associate the visual feedback of hand orientation with the feedback sensation. Afterward, they performed an assessment block comprising 21 trials. Seven orientations, equally distributed between 0° and 180° excluding the extremities (Figure 4), were used as targets and each target was repeated 3 times. The sequence of target positions was randomized while ensuring that the same position was not repeated in succession. Furthermore, the order of target positions was different across conditions. At the beginning of each trial, the controlled hand was placed at the opposite end of the range of motion (0° or 180°) furthest from the target orientation, as shown in Figure 4. In addition, to prevent the subjects from using feedforward control and motivate them to rely on the feedback, the velocity of the prosthesis was changed across trials by multiplying the maximum speed (1.26 rad/s) with a gain randomly selected from the interval 0.4 – 1. The order of conditions was obtained by randomizing the tests with the different number of vibromotors. For the given number of motors (4, 6 or 8), the subjects then tested all σ values in random order. Before switching to the next number of motors, the subject was asked to choose which σ produced the best sensation. Similarly, when all the numbers of motors were tested, the subjects chose the preferred number of vibromotors.

E. Data Analysis

Two outcome measures were used for this study: error and efficiency (Figure 4). The end-point error in orienting the hand (Figure 4, top) was computed as the difference between the final position of the controlled hand and the target position, expressed as the percentage of the range of motion. The end-point error measures how accurately (close to the target) the subject can orient the hand using vibrotactile proprioceptive feedback. In addition, for the given motion speed of the controlled hand in each trial, the path efficiency was calculated as the ratio between the area associated with the optimal trajectory (Figure 4 bottom plot, yellow area, optimal path) and the area associated with the trajectory generated by the subject (Figure 4 bottom plot, green plus yellow area, generated path). The optimal path corresponded to reaching the target orientation from the initial position in one uninterrupted motion at a fixed speed imposed by the TAC test at the beginning of each trial. Therefore, while the literature normally uses only the length of the trajectory [53], the efficacy in the present study was a function of both trajectory and time and was thus computed as the ratio of the respective areas. This parameter is always less or equal to 100% and indicates how much the subject deviated from the optimal path in each feedback condition. These values were calculated for each condition varying the number of vibromotors and the Gaussian σ.

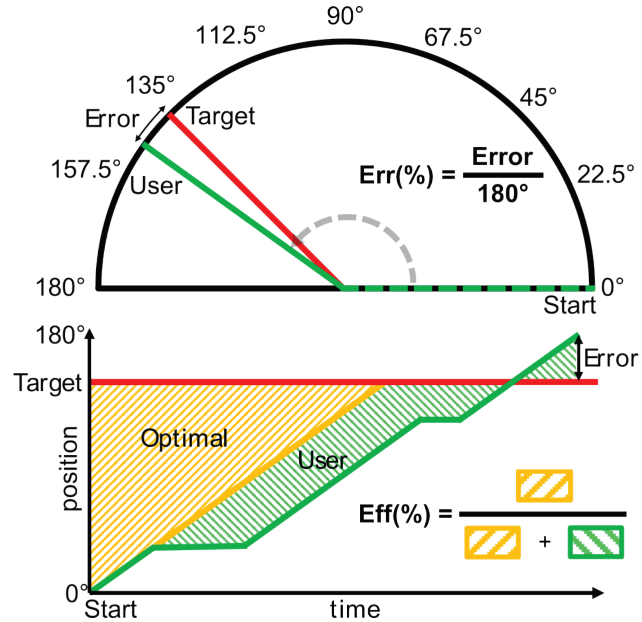

Figure 4 Target positions and outcome measures. The top panel is the error between the target and reached position (control accuracy) and the bottom panel shows the ratio between the area enclosed by the optimal trajectory and the trajectory generated by the subject (control efficiency).

The data were tested for normality using the Shapiro-Wilk test. As the test showed that the data were not normally distributed, the Friedman test was performed, while the post-hoc pairwise comparisons were performed using Wilcoxon signed rank test with Bonferroni correction. OriginPro 2020 Graphic & Analysis (OriginLab Corporation, Northampton, MA, USA) and MATLAB 2020b (The MathWorks, Inc., Natick, MA, USA) were used for the statistical analysis. The average of the outcome measures (error and efficiency) was computed for each subject and condition and compared across conditions.

More specifically, the performance achieved with different σ values was compared for the given number of vibromotors, to test how sensitive were the different number of vibromotors to the modulation of σ. In addition, the performance achieved with different numbers of vibromotors was compared for the given value of σ, to assess whether the number of motors could be reduced without sacrificing the performance.

In addition, the error and efficiency were calculated individually for each target angle. In this case, the angle error and efficiency were calculated by varying the number of vibromotors (averaging across σ), and by varying σ (averaging across the number of vibromotors).

The threshold for statistical significance was set at $p < 0.05$, and outliers were excluded from the statistical comparisons. The results in the text are reported as mean ± standard deviation.

III. Results

The overall results for error and efficiency are summarized in Figure 5, Figure 6, and Figure 7. Figure 5 shows that, in general, an increase in σ leads to a decrease in performance (i.e., an increase in error); however, the impact of σ is less pronounced when the feedback is provided using more motors in the array. This is clearly visible from the 3D bars (Figure 5a)

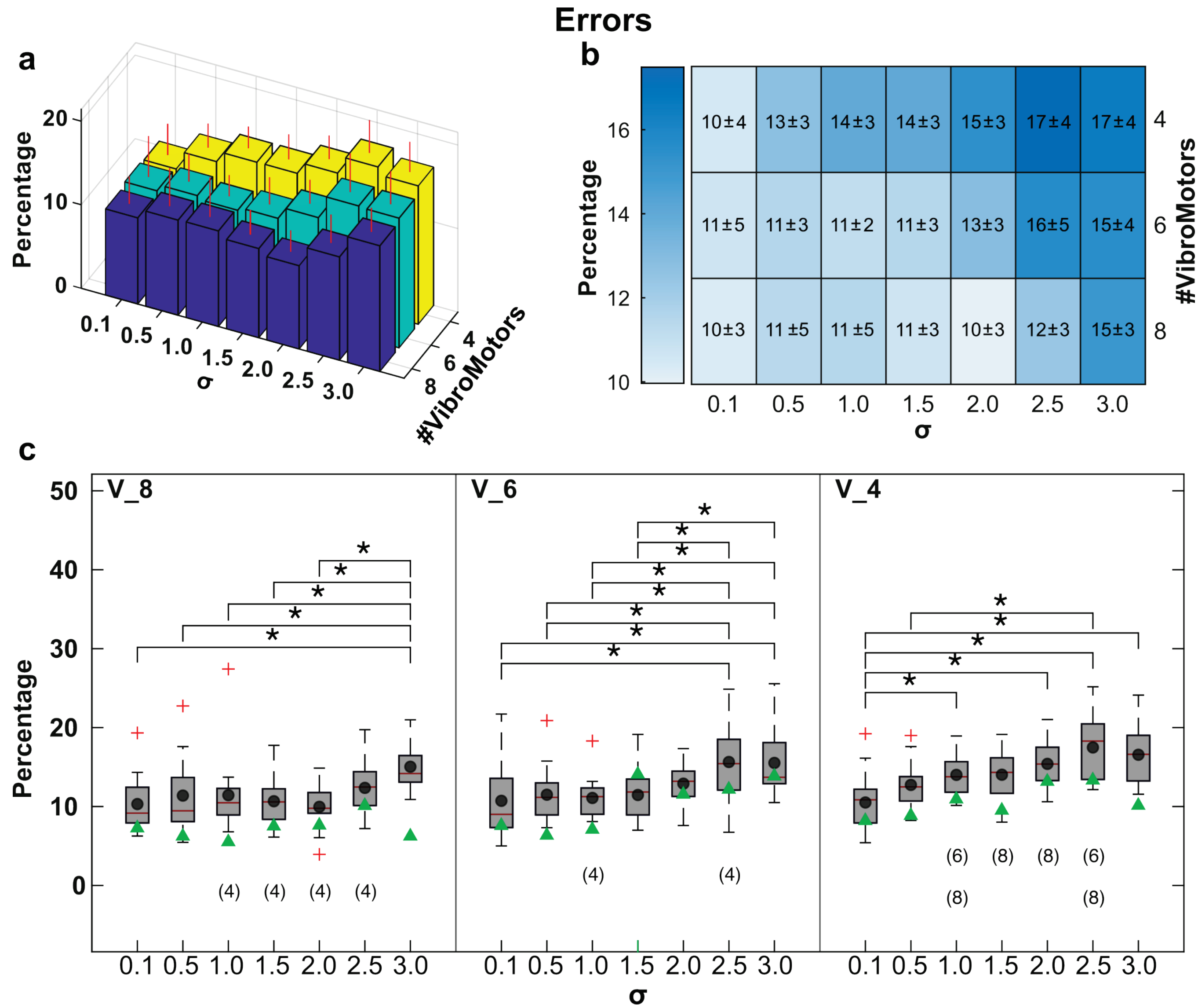

Figure 5 Summary results for the error in the form of: a) bar plot; b) heatmap; and c) boxplots. In the heatmap, a darker color indicates a larger error (lower performance). In the boxplots, V indicates the number of vibromotors, the small circles, and green triangles are the means for the able-bodied subjects and amputee participant, respectively, the red lines indicate the medians, boxes are interquartile ranges, whiskers represent min/max values and crosses are outliers. The horizontal lines denote statistically significant differences for the comparisons across the values of σ for the given number of motors (8, 6, and 4) (*, $p < 0.05$ with Bonferroni correction) while the numbers in parentheses denote statistically significant differences across the number of motors for the given σ.

and heatmap (Figure 5b). For instance, the heatmap has a characteristic diagonal structure, where the area above the diagonal has darker colors (higher errors). As shown in Figure 5c, the performance with 8 and 6 vibromotors was rather resilient to the changes in σ. For 8 motors, the error increased significantly only for the highest value of σ. Specifically, the error for $\sigma = 3.0$ (~15.04 ± 2.9%) was significantly higher than that achieved with all other σ values (~10.7 ± 3.6%) except $\sigma = 2.5$ (~12.4 ± 3.4%). Similar results were obtained with 6 vibromotors where the σ of 2.5 (~15.6 ± 2.9%) was the first value to produce a significant change in performance (~11.5 ± 3.4% for σ of 0.1-2.0). On the contrary, the performance with 4 vibromotors was rather sensitive to the change in σ, and the significant increase in error was registered already for $\sigma = 1.0$ (~14.01 ± 2.6% vs ~11.6 ± 3.3% for σ of 0.1 and 0.5, respectively). When comparing the performance across the number of vibromotors for the given σ, there was no significant difference between 8 and 6 motors for any value of σ, while there was a significant drop in performance for 4 motors. More specifically, the difference arose in the medium range (σ between 1 and 2.5), while in the case of low (0.1 and 0.5) and high (3.0) σ, the error was not significantly different.

Differently from the error, the efficiency (Figure 6) was not significantly affected by σ regardless of the number of motors (~27.4 ± 6.1%, Figure 6c). When comparing across the number of motors, the efficiency with 8 vibromotors was in a few cases significantly higher (~29.2 ± 5.7%) compared to that obtained with 4 vibromotors (~25.7 ± 6.9%), as indicated by the numbers between parentheses in Figure 6c. Again, the trends are particularly visible in the heatmap (Figure 6b). For the efficiency, the heatmap is diagonal but the colour is mirrored compared to that of the errors, indicating that efficiency

This article has been accepted for publication in IEEE Transactions on Biomedical Engineering. This is the author's version which has not been fully edited and content may change prior to final publication. Citation information: DOI 10.1109/TBME.2023.3285850

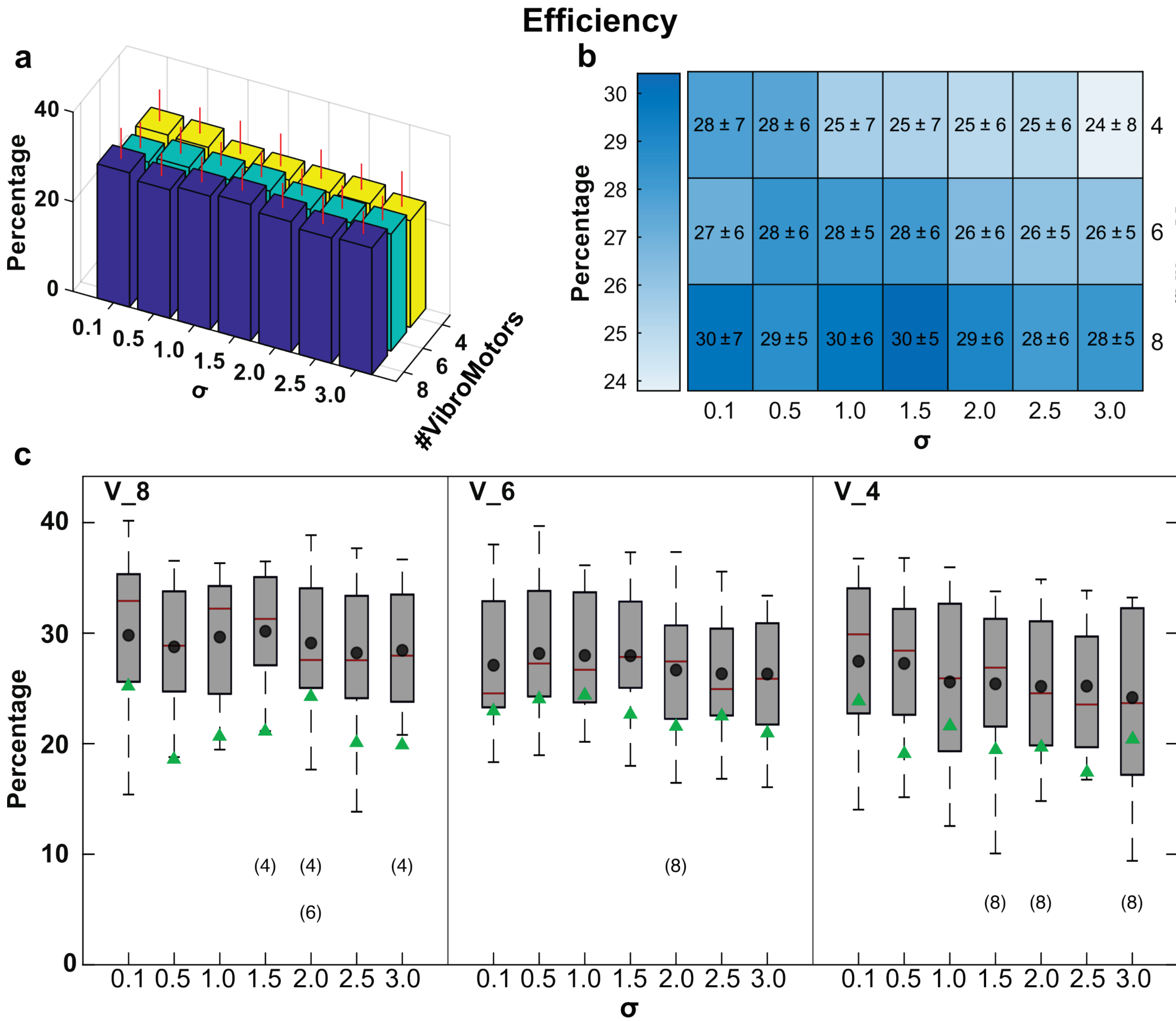

Figure 6 Summary results for efficiency in the form of: a) bar plot; b) heatmap; and c) boxplot. In the heatmap, the darker color indicates higher efficiency (higher performance). In the boxplots, V indicates the number of vibromotors, the small circles, and green triangles are the means for the able-bodied subjects and the amputee participant, respectively, the red lines indicate the medians, boxes are interquartile ranges, whiskers represent min/max values and crosses are outliers. The horizontal lines denote statistically significant differences for the comparisons across the values of σ for the given number of motors (8, 6, and 4) (*, $p < 0.05$ with Bonferroni correction) while the numbers in parentheses denote statistically significant differences between the number of motors for the given σ.

decreased with fewer motors and higher σ (however, as explained, the effect was significant only across the number of motors).

Regarding the amputee subject, the results in both performance measures were within the ranges, and mostly below the mean performance, obtained in able-bodied subjects, as indicated by the green triangles in Figure 5c and Figure 6c. This is an encouraging preliminary result showing that a prospective prosthesis user can successfully interpret and exploit the developed method for control.

Finally, the performance was analyzed for each target angle individually. Figure 7 shows the error (panels a and b) and efficiency (panels c and d) for different target angles grouped by the number of vibromotors (panels a and c) and Gaussian σ (panels b and d). The trends in the heatmaps further support the results presented in Figure 5 and Figure 6, showing that the error generally increased with fewer vibromotors and for higher σ values, while the efficiency was not impacted by those factors. However, Figure 7 reveals that performance depends on the angle. Specifically, for the angles in the middle of the range of motion, the error slightly increased (dark heatmap) while the efficiency decreased (lighted heatmap). We computed the overall error and efficiency averaged over the number of motors and σ and we found that they were 11 ± 7% (error) and 32.3 ± 5% (efficiency) for the extreme positions whereas for the angle of 90° they were 14 ± 6% (error) and 21 ± 8% (efficiency), respectively, and the difference was statistically significant ($p < 0.001$) only for the efficiency.

Regarding subjective preference, most subjects (11) selected 8 vibromotors. Five of them chose $\sigma = 1.0$, three selected $\sigma = 0.5$, two preferred $\sigma = 0.1$ (discrete feedback), and one preferred $\sigma = 1.5$. The remaining subjects chose 4 (2 subjects, $\sigma = 0.5$)

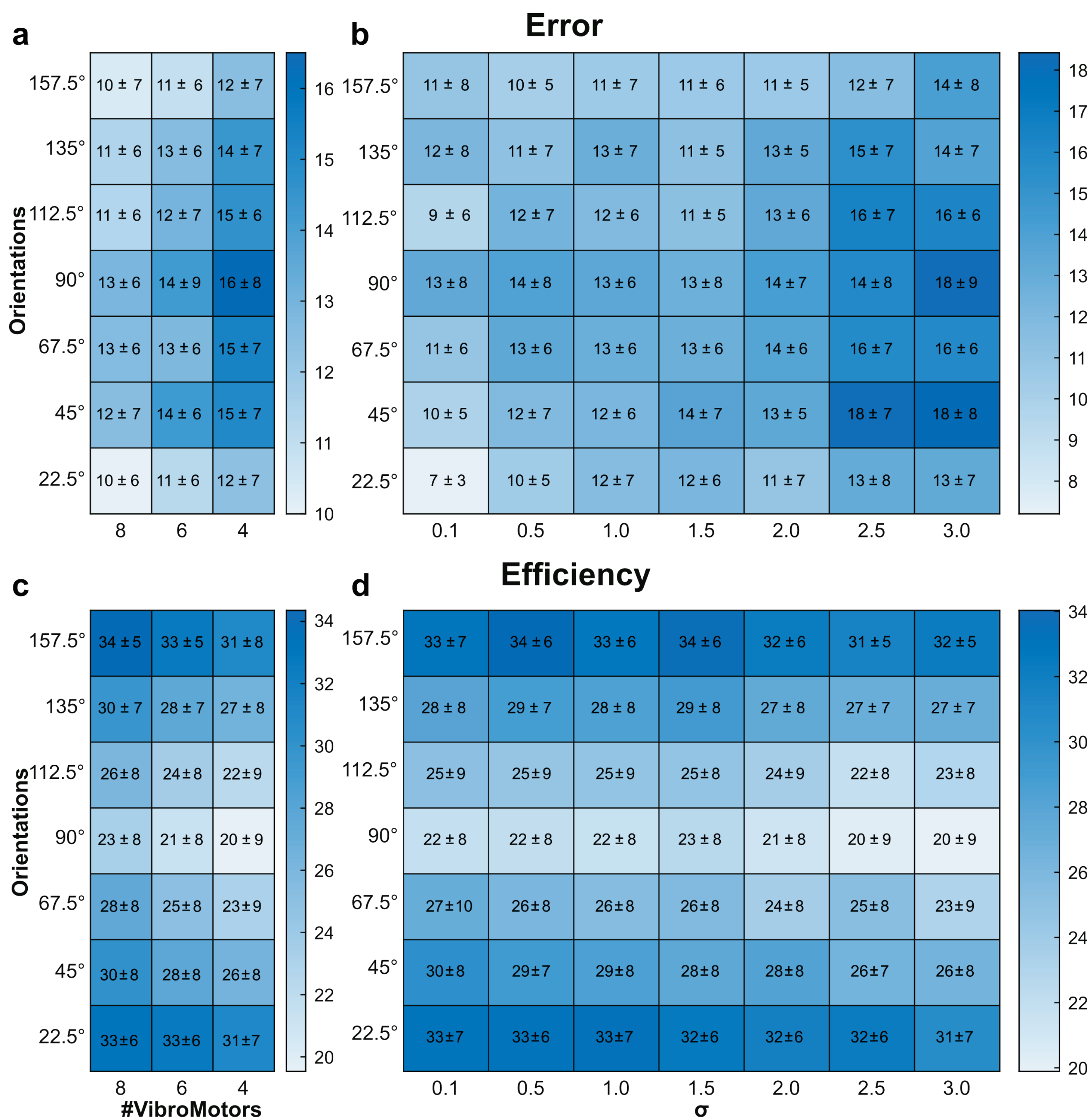

Figure 7 Average performance across the target orientation angles: **a**) Error and c) efficiency for the different number of vibromotors; **b**) Error and d) efficiency for different values of σ.

and 6 motors (2 subjects, σ of 1 and 1.5, respectively). The amputee participant preferred 8 vibromotors with a σ of 1.0.

IV. Discussion

The present study proposed a novel approach to convey proprioceptive information that can be flexibly configured by adjusting the smoothness of the moving sensation (σ) and the number of vibromotors used. Most of the methods in the literature assume a single configuration based on heuristically selected parameters, while the present study systematically explored the parameter space of the proposed method and provides important insights for its successful application. The main conclusions of the experimental assessment are: 1) discrete feedback consistently showed high performance regardless of the number of motors; 2) nevertheless, with enough motors, the smoothness of feedback can be increased over a broad range without impacting the localization of sensation; 3) the subjects prefer smooth rather than discrete feedback; and 4) the number of motors can be safely decreased from 8 to 6 and, if smoothness is not the priority, even to 4. Importantly, the second point additionally reveals that σ might be used not only to adjust the smoothness but possibly as an extra "degree of freedom" to convey another feedback variable, as discussed later. Overall, the novel method allowed an effective closed-loop control (average error < 10% for some parameter combinations) in able-bodied as well as in an amputee subject. Although the method was used to convey wrist rotation, other variables could be transmitted using identical mapping via a circular or linear array (e.g., aperture and grasping force). Therefore, the key contribution of the present study is an effective feedback approach that can be flexibly customized in terms of sensation quality and potentially the nature and the number of feedback variables, according to the requirements of an application and/or user preference. The aforementioned outcomes are further discussed below in dedicated paragraphs.

The results demonstrated that the Gaussian interpolation of intensity is an effective method to generate smoothly moving sensations around the forearm. When enough motors were available in the array (8 and 6), the amount of smoothing set by the value of σ could be modulated substantially without significant impact on performance (Figure 5b and d). Therefore, the spread of sensation did not negatively affect the subject's ability to locate the peak of intensity and thereby determine the associated wrist orientation.

The possibility of modulating σ without significant impact on the ability to locate the peak of sensation is an important result for the application of this feedback approach. First, this means that the value of σ can be selected based on the subject's preference. The subject can choose the feedback configuration with more or less spreading and/or continuity in transition. Indeed, when asked to indicate their preference, in most cases, the subjects indicated that they prefer smooth rather than discrete feedback, selecting different values of σ in the low to medium range, namely, from 0.5 to 1.5. Second, since σ does not affect the perception of rotation, this parameter could be used to encode an additional variable, for instance, hand aperture. Increasing σ spreads the sensation around the forearm, resembling thereby the movement of the hand enclosing an object. Such encoding would therefore allow for a compact solution, where the same interface could be used to provide the simultaneous feedback of wrist rotation and hand aperture. However, the results also show that this approach would work only with enough motors in the array. With 4 motors, for instance, the range in which σ can be modulated without affecting the performance is narrow. Hence, in the case of a small number of vibromotors, it could be challenging for the subject to clearly perceive the change in the feedback variable associated with σ.

Decreasing the number of motors required to provide feedback is an important advantage for the envisioned clinical application. Our experimental results showed that the number of motors can be decreased from 8 to 6 while still maintaining both the smoothness of the feedback (higher σ) and the performance. The number of vibromotors can be reduced even to 4 if the participant can "tolerate" discrete sensations (smaller σ). Fewer motors reduce the complexity of the interface, which can improve robustness and simplify the integration of the feedback into the socket. The present results demonstrate that there is a tradeoff between the value of σ and the number of motors, where the former parameter puts a limit on how many vibromotors can be decreased without incurring a significant loss of performance. For low values of σ (0.1 and 0.5), the number of vibromotors (i.e., feedback interface) can be halved, from 8 to 4, while $\sigma > 0.5$ allows only a smaller reduction (from 8 to 6).

Our initial assumption was that the small σ would be more sensitive to the decrease in the number of motors. Small σ (0.1) produced discrete feedback that jumps from motor to motor (no interpolation across motors), and hence, with fewer motors, the feedback resolution is presumably lower. Contrary to our assumption, the subjects achieved good results with small σ even when using only 4 motors. The expression (1) that was used to generate the intensity introduced a brief period of no stimulation when changing between the neighboring motors, and we believe that this cue allowed the subjects to effectively increase the feedback resolution. Nevertheless, such a stimulation pattern was not intuitively related to the prosthesis movements (discrete feedback vs. continuous rotation). This was confirmed by the qualitative, subjective outcomes, as most subjects selected at least some level of interpolation, even when using 8 motors. The interpolation produced continuous sensation around the forearm by generating virtual tactile points between the motors. However, it seemed that this approach needed a certain minimal number of motors to be effective (8 and 6 vs. 4). Finally, the amount of interpolation can be also excessive, as the highest values of σ (2.5 and 3) produced a blurred sensation that confused the perception of the continuous movement around the forearm. Indeed, the highest values of σ decreased the performance regardless of the number of motors.

The overall recommendation for the configuration of the proposed feedback interface, therefore, depends on the weighing of the subjective versus objective factors. If priority is given to the subjects' preference, 8 motors should be used with a medium level of interpolation (smooth sensation). However, if there is a need to decrease the number of motors in the array, 6 motors could be used with a similar amount of interpolation to maintain both the continuity of sensation and closed-loop performance.

The results obtained for each target angle (Figure 7) show that it was more difficult for the subjects to adjust the wrist orientation for the positions towards the middle of the range of motion (ROM). This is an intuitive result because the subjects could use the positions at the end of ROM as the well-defined anchors since the stimulation stopped changing when the subject reached the ROM end.

The next step in this research will be to expand the proposed approach to implement the proprioceptive feedback for all DoFs of a multifunctional prosthetic hand. As explained above, the second DoF can be added by exploiting the presumed "independence" of the two parameters (Gaussian profile peak and σ), i.e., using σ to encode the hand aperture simultaneously with the rotation of the wrist. To accommodate more DoFs (e.g., wrist flexion/extension and force), however, additional motors need to be added.

The proprioceptive feedback was already employed for prosthesis control [36, 37, 63], but not in the form presented in this study, where Gaussian interpolation was combined with spatial encoding to produce the sensation of continuous movement around the forearm. A previous study used the principle of generating phantom sensations [46] and also reported good results with 6 motors. However, they employed a fixed number of motors, discrete activation (instead of Gaussian interpolation) thereby producing discrete sensations, and the application was wrist guidance and not prosthesis control.

The present experiment was performed by controlling a virtual prosthesis via keyboard using the contralateral hand, as the focus was on comparing the feedback parameters. However, in the envisioned practical application, both control and feedback will be performed ipsilaterally, and this could affect the effectiveness of feedback (e.g., forearm movements and muscle activation can impact the perception of sensations). The placement of a feedback interface was investigated in a recent study, albeit in a different context (control of balance), and the results demonstrated that the placement can be indeed an important factor [64]. Therefore, the next step in this research will be to test the interaction between feedback and pattern classification control in both able-bodied and amputee subjects. Importantly, the results of the present study will inform the design of the feedback (parameter selection) for this future assessment.

The aim of the present study was not a direct clinical translation but a systematic investigation of the novel feedback scheme and the effect of its parameters on the performance of closed-loop control, i.e., wrist rotation using an ideal command interface and the novel feedback method. Nevertheless, the results obtained in an amputee who could use the feedback as effectively as able-bodied subjects are encouraging from the viewpoint of future clinical translation.

V. Conclusion

The present study is the first effort to investigate the application of a novel feedback scheme that combines spatial encoding with Gaussian interpolation to provide continuous proprioceptive sensation for wrist rotation in prosthetic applications. The quality of the produced sensation, namely, the location of the peak intensity and the amount of spreading, depends on the number of vibromotors used in the array and the value of the parameter σ of the Gaussian interpolation profile. Overall, the present study has shown that the novel approach provided clear rotational feedback that was easy to interpret and use for closed-loop control. Nevertheless, there was a clear preference for a higher number of vibromotors (8 and 6). An increased number of vibromotors was also more robust with respect to the change in σ, i.e., the amount of spreading of sensation (continuity of the feedback) could be increased to higher values without the decrease in performance. This is an important outcome for the application of proprioceptive feedback, as it points out that the spatial modulation and σ could be used to simultaneously encode two feedback variables using a compact solution (i.e., an array of vibromotors).

VI. Acknowledgment

The authors thank Lorenzo Lombardi, Astrid Florio, and Paolo Rossi for their contribution to the development and assembly of the custom boards used in this study. We also thank the Hannes project team for their cooperation during the development of this system.

VII. References

[1] C. Antfolk, A. Björkman, S.-O. Frank, F. Sebelius, G. Lundborg, and B. Rosen, "Sensory feedback from a prosthetic hand based on air-mediated pressure from the hand to the forearm skin," *Journal of rehabilitation medicine,* vol. 44, no. 8, pp. 702-707, 2012.

[2] A. Marinelli *et al.*, "Active upper limb prostheses: A review on current state and upcoming breakthroughs," *Progress in Biomedical Engineering,* 2022.

[3] H. Shahsavari *et al.*, "Upper limb amputation; Care needs for reintegration to life: An integrative review," *International journal of orthopaedic and trauma nursing,* vol. 38, p. 100773, 2020.

[4] S. Salminger *et al.*, "Current rates of prosthetic usage in upper-limb amputees–have innovations had an impact on device acceptance?," *Disability and Rehabilitation,* pp. 1-12, 2020.

[5] M. A. Wilke, C. Niethammer, B. Meyer, D. Farina, and S. Dosen, "Psychometric characterization of incidental feedback sources during grasping with a hand prosthesis," *Journal of neuroengineering and rehabilitation,* vol. 16, no. 1, pp. 1-13, 2019.

[6] M. Markovic, M. A. Schweisfurth, L. F. Engels, D. Farina, and S. Dosen, "Myocontrol is closed-loop control: incidental feedback is sufficient for scaling the prosthesis force in routine grasping," *Journal of neuroengineering and rehabilitation,* vol. 15, no. 1, pp. 1-11, 2018.

[7] J. W. Sensinger and S. Dosen, "A review of sensory feedback in upper-limb prostheses from the perspective of human motor control," *Frontiers in Neuroscience,* vol. 14, 2020.

[8] F. Clemente *et al.*, "Intraneural sensory feedback restores grip force control and motor coordination while using a prosthetic hand," *Journal of neural engineering,* vol. 16, no. 2, p. 026034, 2019.

[9] G. Valle *et al.*, "Biomimetic intraneural sensory feedback enhances sensation naturalness, tactile sensitivity, and manual dexterity in a bidirectional prosthesis," *Neuron,* vol. 100, no. 1, pp. 37-45. e7, 2018.

[10] M. Markovic *et al.*, "The clinical relevance of advanced artificial feedback in the control of a multi-functional myoelectric prosthesis," *Journal of neuroengineering and rehabilitation,* vol. 15, no. 1, pp. 1-15, 2018.

[11] G. Di Pino *et al.*, "Sensory-and action-oriented embodiment of neurally-interfaced robotic hand prostheses," *Frontiers in Neuroscience,* vol. 14, p. 389, 2020.

[12] A. W. Shehata, M. Rehani, Z. E. Jassat, and J. S. Hebert, "Mechanotactile sensory feedback improves embodiment of a prosthetic hand during active use," *Frontiers in neuroscience,* vol. 14, p. 263, 2020.

[13] S. Raspopovic, G. Valle, and F. M. Petrini, "Sensory feedback for limb prostheses in amputees," *Nature Materials,* pp. 1-15, 2021.

[14] P. Svensson, U. Wijk, A. Björkman, and C. Antfolk, "A review of invasive and non-invasive sensory feedback in upper limb prostheses," *Expert review of medical devices,* vol. 14, no. 6, pp. 439-447, 2017.

[15] C. Antfolk, M. D'alonzo, B. Rosén, G. Lundborg, F. Sebelius, and C. Cipriani, "Sensory feedback in upper limb prosthetics," *Expert review of medical devices,* vol. 10, no. 1, pp. 45-54, 2013.

[16] I. Cuberovic, A. Gill, L. J. Resnik, D. J. Tyler, and E. L. Graczyk, "Learning of artificial sensation through long-term home use of a sensory-enabled prosthesis," *Frontiers in neuroscience,* vol. 13, p. 853, 2019.

[17] M. M. Iskarous and N. V. Thakor, "E-skins: Biomimetic sensing and encoding for upper limb prostheses," *Proceedings of the IEEE,* vol. 107, no. 10, pp. 2052-2064, 2019.

[18] S. Raspopovic, G. Valle, and F. M. Petrini, "Sensory feedback for limb prostheses in amputees," *Nature Materials,* vol. 20, no. 7, pp. 925-939, 2021.

[19] E. D'Anna *et al.*, "A closed-loop hand prosthesis with simultaneous intraneural tactile and position feedback," *Science Robotics,* vol. 4, no. 27, p. eaau8892, 2019.

[20] S. Micera *et al.*, "Decoding information from neural signals recorded using intraneural electrodes: toward the development of a neurocontrolled hand prosthesis," *Proceedings of the IEEE,* vol. 98, no. 3, pp. 407-417, 2010.

[21] C. M. Oddo *et al.*, "Intraneural stimulation elicits discrimination of textural features by artificial fingertip in intact and amputee humans," *elife,* vol. 5, p. e09148, 2016.

[22] G. K. Patel, S. Dosen, C. Castellini, and D. Farina, "Multichannel electrotactile feedback for simultaneous and proportional myoelectric control," *Journal of neural engineering,* vol. 13, no. 5, p. 056015, 2016.

[23] M. Štrbac *et al.*, "Integrated and flexible multichannel interface for electrotactile stimulation," *Journal of neural engineering,* vol. 13, no. 4, p. 046014, 2016.

[24] S. Dosen *et al.*, "Multichannel electrotactile feedback with spatial and mixed coding for closed-loop control of grasping force in hand prostheses," *IEEE Transactions on Neural Systems and Rehabilitation Engineering,* vol. 25, no. 3, pp. 183-195, 2016.

[25] F. Clemente, M. D'Alonzo, M. Controzzi, B. B. Edin, and C. Cipriani, "Non-invasive, temporally discrete feedback of object contact and release improves grasp control of closed-loop myoelectric transradial prostheses," *IEEE Transactions on Neural Systems and Rehabilitation Engineering,* vol. 24, no. 12, pp. 1314-1322, 2015.

[26] E. D'Anna *et al.*, "A closed-loop hand prosthesis with simultaneous intraneural tactile and position feedback," *Science Robotics,* vol. 4, no. 27, 2019.

[27] L. E. Osborn *et al.*, "Prosthesis with neuromorphic multilayered e-dermis perceives touch and pain," *Science robotics,* vol. 3, no. 19, 2018.

[28] K. Horch, S. Meek, T. G. Taylor, and D. T. Hutchinson, "Object discrimination with an artificial hand using electrical stimulation of peripheral tactile and proprioceptive pathways with intrafascicular electrodes," *IEEE Transactions on Neural Systems and Rehabilitation Engineering,* vol. 19, no. 5, pp. 483-489, 2011.

[29] F. Cordella *et al.*, "Literature review on needs of upper limb prosthesis users," *Frontiers in neuroscience,* vol. 10, p. 209, 2016.

[30] A. D. Roche, B. Lakey, I. Mendez, I. Vujaklija, D. Farina, and O. C. Aszmann, "Clinical Perspectives in Upper Limb Prostheses: An Update," *Current Surgery Reports,* 2019.

[31] M. N. Nemah, O. H. Aldulaymi, C. Y. Low, N. A. C. Zakaria, and S. Mohamaddan, "A hybrid haptic feedback stimulation device to recover the missing sensation of the upper limb amputees," in *IOP Conference Series: Materials Science and Engineering*, 2020, vol. 834, no. 1: IOP Publishing, p. 012013.

[32] C. Antfolk *et al.*, "Artificial redirection of sensation from prosthetic fingers to the phantom hand map on transradial amputees: vibrotactile versus mechanotactile sensory feedback," *IEEE transactions on neural systems and rehabilitation engineering,* vol. 21, no. 1, pp. 112-120, 2012.

[33] P. Mamidanna, J. L. Dideriksen, and S. Dosen, "The impact of objective functions on control policies in closed-loop control of grasping force with a myoelectric prosthesis," *Journal of Neural Engineering,* vol. 18, no. 5, p. 056036, 2021.

[34] A. M. De Nunzio *et al.*, "Tactile feedback is an effective instrument for the training of grasping with a prosthesis at low-and medium-force levels," *Experimental brain research,* vol. 235, no. 8, pp. 2547-2559, 2017.

[35] R. M. Mayer *et al.*, "Tactile feedback in closed-loop control of myoelectric hand grasping: conveying information of multiple sensors simultaneously via a single feedback channel," *Frontiers in Neuroscience,* vol. 14, p. 348, 2020.

[36] M. A. Garenfeld, C. K. Mortensen, M. Strbac, J. L. Dideriksen, and S. Dosen, "Amplitude versus spatially modulated electrotactile feedback for myoelectric control of two degrees of freedom," *Journal of Neural Engineering,* vol. 17, no. 4, p. 046034, 2020.

[37] O. Kayhan, A. K. Nennioglu, and E. Samur, "A skin stretch tactor for sensory substitution of wrist proprioception," in *2018 IEEE Haptics Symposium (HAPTICS)*, 2018: IEEE, pp. 26-31.

[38] E. Battaglia, J. P. Clark, M. Bianchi, M. G. Catalano, A. Bicchi, and M. K. O'Malley, "Skin stretch haptic feedback to convey closure information in anthropomorphic, under-actuated upper limb soft prostheses," *IEEE Transactions on Haptics,* vol. 12, no. 4, pp. 508-520, 2019.

[39] L. Vargas, H. Huang, Y. Zhu, and X. Hu, "Object Recognition via Evoked Sensory Feedback during Control of a Prosthetic Hand," *IEEE Robotics and Automation Letters,* vol. 7, no. 1, pp. 207-214, 2021.

[40] H. Cha, S. An, S. Choi, S. Yang, S. Park, and S. Park, "Study on Intention Recognition and Sensory Feedback: Control of Robotic Prosthetic Hand through EMG Classification and Proprioceptive Feedback using Rule-based Haptic Device," *IEEE Transactions on Haptics,* 2022.

[41] A. Blank, A. M. Okamura, and K. J. Kuchenbecker, "Identifying the role of proprioception in upper-limb prosthesis control: Studies on targeted motion," *ACM Transactions on Applied Perception (TAP),* vol. 7, no. 3, pp. 1-23, 2008.

[42] P. D. Marasco *et al.*, "Neurorobotic fusion of prosthetic touch, kinesthesia, and movement in bionic upper limbs promotes intrinsic brain behaviors," *Science Robotics,* vol. 6, no. 58, p. eabf3368, 2021.

[43] M. Rossi, M. Bianchi, E. Battaglia, M. G. Catalano, and A. Bicchi, "HapPro: a wearable haptic device for proprioceptive feedback," *IEEE Transactions on Biomedical Engineering,* vol. 66, no. 1, pp. 138-149, 2018.

[44] R. W. Mann and S. D. Reimers, "Kinesthetic Sensing for the EMG Controlled" Boston Arm"," *IEEE Transactions on Man-Machine Systems,* vol. 11, no. 1, pp. 110-115, 1970.

[45] A. E. Pena, L. Rincon-Gonzalez, J. J. Abbas, and R. Jung, "Effects of vibrotactile feedback and grasp interface compliance on perception and control of a sensorized myoelectric hand," *PloS one,* vol. 14, no. 1, p. e0210956, 2019.

[46] J. V. S. Luces, K. Okabe, Y. Murao, and Y. Hirata, "A phantom-sensation based paradigm for continuous vibrotactile wrist guidance in two-dimensional space," *IEEE Robotics and Automation Letters,* vol. 3, no. 1, pp. 163-170, 2017.

[47] L. Vargas, H. H. Huang, Y. Zhu, and X. Hu, "Closed-loop control of a prosthetic finger via evoked proprioceptive information," *Journal of Neural Engineering,* vol. 18, no. 6, p. 066029, 2021.

[48] R. Yunus *et al.*, "Development and testing of a wearable vibrotactile haptic feedback system for proprioceptive rehabilitation," *IEEE Access,* vol. 8, pp. 35172-35184, 2020.

[49] H. J. Witteveen, H. S. Rietman, and P. H. Veltink, "Vibrotactile grasping force and hand aperture feedback for myoelectric forearm prosthesis users," *Prosthetics and orthotics international,* vol. 39, no. 3, pp. 204-212, 2015.

[50] M. A. Garenfeld *et al.*, "A compact system for simultaneous stimulation and recording for closed-loop myoelectric control," *Journal of NeuroEngineering and Rehabilitation,* vol. 18, no. 1, pp. 1-17, 2021.

[51] A. Erwin and F. C. Sup IV, "A haptic feedback scheme to accurately position a virtual wrist prosthesis using a three-node tactor array," *PloS one,* vol. 10, no. 8, p. e0134095, 2015.

[52] S.-W. Shim and H. Z. Tan, "palmScape: Calm and pleasant vibrotactile signals," in *International Conference on Human-Computer Interaction*, 2020: Springer, pp. 532-548.

[53] M. Ortiz-Catalan, B. Håkansson, and R. Brånemark, "Real-time and simultaneous control of artificial limbs based on pattern recognition algorithms," *IEEE Transactions on Neural Systems and Rehabilitation Engineering,* vol. 22, no. 4, pp. 756-764, 2014.

[54] M. Laffranchi *et al.*, "The Hannes hand prosthesis replicates the key biological properties of the human hand," *Science Robotics,* 2020.

[55] D. Di Domenico *et al.*, "Hannes Prosthesis Control Based on Regression Machine Learning Algorithms," presented at the 2021 IEEE/RSJ International Conference on Intelligent Robots and Systems (IROS 2021), 2021.

[56] A. Marinelli *et al.*, "Miniature EMG Sensors for Prosthetic Applications," in *2021 10th International IEEE/EMBS Conference on Neural Engineering (NER)*, 2021: IEEE, pp. 1022-1025.

[57] A. Marinelli *et al.*, "Performance Evaluation of Pattern Recognition Algorithms for Upper Limb Prosthetic Applications," in *8th IEEE RAS/EMBS International Conference for Biomedical Robotics and Biomechatronics (BioRob)*, 2020: IEEE.

[58] M. Solomonow, J. Lyman, and A. Freedy, "Electrotactile two-point discrimination as a function of frequency, body site, laterality, and stimulation codes," *Annals of biomedical engineering,* vol. 5, no. 1, pp. 47-60, 1977.

[59] I. Vybronics. "VC0625B001L." https://www.vybronics.com/wp-content/uploads/datasheet-files/Vybronics-VC0625B001L-datasheet.pdf (accessed.

[60] S. Gilman, "Joint position sense and vibration sense: Anatomical organisation and assessment," *Journal of neurology, neurosurgery, and psychiatry,* vol. 73, pp. 473-7, 12/01 2002, doi: 10.1136/jnnp.73.5.473.

[61] N. Prins, *Psychophysics: a practical introduction*. Academic Press, 2016.

[62] D. G. Buma, J. R. Buitenweg, and P. H. Veltink, "Intermittent stimulation delays adaptation to electrocutaneous sensory feedback," *IEEE Transactions on Neural Systems and Rehabilitation Engineering,* vol. 15, no. 3, pp. 435-441, 2007.

[63] F. S. di Luzio, C. Lauretti, F. Cordella, F. Draicchio, and L. Zollo, "Visual vs vibrotactile feedback for posture assessment during upper-limb robot-aided rehabilitation," *Applied ergonomics,* vol. 82, p. 102950, 2020.

[64] J. Azbell, J. Park, S.-H. Chang, M. P. Engelen, and H. Park, "Plantar or palmar tactile augmentation improves lateral postural balance with significant influence from cognitive load," *IEEE Transactions on Neural Systems and Rehabilitation Engineering,* vol. 29, pp. 113-122, 2020.